Resonance Raman Study of the Short-Time Photodissociation Dynamics of the A-Band Absorption of Cyclopropyl Iodide in Cyclohexane Solution†

Xuming Zheng,*,‡ Yun-Liang Li,§ and David Lee Phillips*,§

Department of Applied Chemistry, Zhejiang Institute of Science and Technology, 88 Wenyi Road, Hangzhou 310033, P. R. China, and Department of Chemistry, The University of Hong Kong, Pokfulam Road, Hong Kong S.A.R., P. R. China

Received: February 17, 2004; In Final Form: April 14, 2004

Resonance Raman spectra were obtained for cyclopropyl iodide in cyclohexane solution with excitation wavelengths in resonance with the A-band absorption spectrum. These spectra indicate that the Franck−Condon region photodissociation dynamics have multidimensional character with motion mainly along the nominal C−I stretch and nominal C−C−I deformation normal modes accompanied by moderate motion along the nominal cyclopropyl ring breathing and ring deformation normal modes. A preliminary resonance Raman intensity analysis was done, and the results for cyclopropyl iodide were compared to previously reported results for several cyclic and noncyclic alkyl iodides.

Introduction

The A-band absorption (~260 nm) of alkyl iodides has long been examined as a model for direct photodissociation reactions.[1−43] Many experimental and theoretical investigations have been done to examine the photodissociation dynamics, the energy disposal, the branching ratio of the $^3Q_0$ and $^1Q_1$ curve crossing, etc. of the direct photodissociation reactions of alkyl iodides.[1−41] However, there have not been a large number of investigations of the effect of geometrical conformation and ring strain on the dynamics and energy disposal of A-band photodissociation of cyclic alkyl iodides.

A time-of-flight photofragment translational spectroscopy investigation of the A-band cyclohexyl iodide photodissociation yielded the translational energy distributions of the I* and I fragments. This experiment observed that the axial conformer gets 6.0 ± 0.8 kcal/mol more translational energy than the equatorial conformer.[42] This suggests that the cyclohexyl radical generated from the equatorial conformation A-band photodissociation gets more internal excitation than the cyclohexyl radicals made from the axial conformation photodissociation. A resonance Raman study of the A-band short-time photodissociation dynamics of the equatorial conformer of cyclohexyl iodide determined that the initial C−I bond length changes upon photoexcitation,[43] and these results suggest that the cyclohexyl radical receives substantial internal excitation,[43] consistent with the time-of-flight photofragment translational spectroscopy experiments.[42] Comparison of the short-time photodissociation dynamics results for A-band cyclohexyl iodide with previous results for several noncyclic alkyl iodides[40] suggested that the geometry of the C−I bond relative to the plane of the α-, β- and γ-carbon atoms of the cyclohexyl group appears to be important in determining the degree of internal excitation of the cyclohexyl fragment.[43] These experimental time-of-flight photofragment spectroscopy and resonance Raman spectroscopy results[42,43] indicate that the two different geometrical conformations (axial and equatorial) of cyclohexyl iodide have noticeably different photodissociation dynamics and energy disposal. Similar results were obtained from a resonance Raman study of the axial and equatorial conformers of cyclopentyl iodide.[44]

Single bond rotational conformers have also been examined for *n*-propyl iodide A-band photodissociation (gas and solution phases).[40] The resonance Raman study found that the trans and gauche conformers of *n*-propyl iodide have noticeably different multidimensional short-time photodissociation dynamics. These different dynamics can be mostly attributed to the position of the C−I bond relative to the plane of the three carbon atoms of the *n*-propyl group in *n*-propyl iodide.[40] Molecular beam experimental results suggested that the *n*-propyl radicals produced from the A-band photodissociation of trans and gauche conformations of *n*-propyl iodide had similar broad translational energy distributions.[4] But, the different short-time photodissociation dynamics for the trans and gauche conformations of *n*-propyl iodide[40] suggests the energy disposal is probably spread among substantially different distributions among the internal degrees of freedom for the *n*-propyl radicals produced from the trans and gauche conformers of *n*-propyl iodide.

In this paper, we investigate the short-time photodissociation dynamics of the main transition associated with the A-band absorption of cyclopropyl iodide in cyclohexane solution. The cyclic ring strain and initial C−C−C bond angles for cyclopropyl iodide are significantly different than in cyclohexyl iodide and cyclopentyl iodide. This would allow a comparison of how the ring strain and initial C−C−C geometry may influence or affect the short-time photodissociation dynamics in cyclic alkyl iodides. In addition, we can also compare the results for cyclopropyl iodide to the previously studied conformers of *n*-propyl iodide to examine the differences and/or similarities between C−I bond cleavage in a cyclic versus a noncyclic chain alkyl iodide. We also note that cyclopropyl iodide A-band photodissociation in the gas and solution phases has received attention for investigating possible reactions involving surface intersections between open shell and closed shell potential

† Part of the special issue "Richard Bersohn Memorial Issue".

* To whom correspondence should be addressed. Telephone: 852-2859-2160 (D.L.P.). FAX: 852-2857-1586 (D.L.P.) or 86-0571-8074072 (X.Z.). E-mail: phillips@hkucc.hku.hk (D.L.P.) or xzheng@mail.hz.zj.cn (X.Z.).

‡ Zhejiang Institute of Science and Technology.

§ The University of Hong Kong.

10.1021/jp0492772 CCC: $27.50
Published on Web 05/22/2004

energy surfaces to explain the formation of an allyl radical product.[45] Arnold et al.[45] recently proposed that in the first surface crossing, the cyclopropyl radical and iodine atom (open shell) initially produced from the photodissociation of cyclopropyl iodide can undergo some charge separation to make a cation−iodide ion pair (closed shell) that can then change into an allyl cation−iodide ion pair (closed shell), and then in the second surface crossing, the back-electron transfer between the allyl cation−iodide ion pair allows the final formation of an allyl radical and iodide atom (open shell) observed in their experiments.[45] The resonance Raman spectra of cyclopropyl iodide will also allow us to examine the Franck−Condon region dynamics following A-band excitation of cyclopropyl iodide, and these results will be briefly discussed in relation to this proposed mechanism.

Experimental and Computational Methods

FT-IR, FT-Raman, and Resonance Raman Experiments. Cyclopropyl iodide was synthesized using previously reported methods[45] and the purity of the sample was determined using NMR and UV/vis spectroscopies. The FT-IR spectrum of cyclopropyl iodide in neat liquid was acquired with 2 cm^{-1} resolution (Perkin-Elmer 1 FT-IR spectrometer). The FT-Raman spectrum of neat liquid cyclopropyl iodide was obtained with 2 cm^{-1} resolution and 532 nm excitation (Thermo Nicolet Almega Dispersive Raman spectrometer).

The resonance Raman experiments used concentrations in the 0.10−0.15 M range for cyclopropyl iodide in cyclohexane solvent. The methods and experimental apparatus used for the resonance Raman experiments has been described elsewhere,[35−41,43,44] so only a short account will be given here. The harmonics of a nanosecond Nd:YAG laser and their hydrogen Raman shifted laser lines supplied the excitation wavelengths used in the resonance Raman experiments. The excitation laser beam was loosely focused to about a 0.5 mm diameter spot size onto a flowing liquid stream of sample. A backscattering geometry was used for sample excitation and for collection of the Raman scattered light by reflective optics. The Raman scattered light was imaged through a polarizer and entrance slit of a 0.5 m spectrograph whose grating dispersed the light onto a liquid nitrogen cooled CCD mounted on the exit of the spectrograph. The CCD acquired the Raman signal for about 90−120 s before being read out to an interfaced PC computer. About 10−30 of these scans were summed to obtain the resonance Raman spectrum. The Raman shifts of the resonance Raman spectra were calibrated using the known vibrational frequencies of the cyclohexane solvent Raman bands. The solvent Raman bands were subtracted from the resonance Raman spectra using an appropriately scaled solvent spectrum. Spectra of an intensity calibrated deuterium lamp were used to correct the resonance Raman spectral intensities for the variation in detection efficiency as a function of wavelength. Portions of the resonance Raman spectra were fit to a baseline plus a sum of Lorentzian bands to obtain the integrated areas of the Raman bands.

The absolute Raman cross sections of the cyclopropyl iodide resonance Raman spectra were determined relative to the 802 cm^{-1} Raman band of the cyclohexane solvent. An ultraviolet/visible (UV/vis) spectrometer was used to determine the concentrations of the cyclopropyl iodide sample before and after each measurement, and the absorption spectra changed by <5% due to photodecomposition and/or solvent evaporation. The absolute Raman cross sections were computed by using the average concentration before and after three measurements and by finding the mean of three trials to get a final value for the excitation wavelengths determined.

Time-Dependent Wave Packet Calculations To Model the Resonance Raman Intensities and Absorption Spectrum and Density Functional Theory Calculations. A simple model and wave packet calculations were used to simulate the absorption spectrum and resonance Raman intensities of the more intense A-band resonance Raman spectra. These calculations and model are not intended to be a complete description of the spectra but are used to investigate the main features of the short-time photodissociation dynamics of cyclopropyl iodide. We note that resonance Raman intensity analysis has proven to be a useful method for characterizing the Franck−Condon region potential energy surfaces and dynamics associated with many types of electronic transitions,[35−41,46−53] including those associated with direct photodissociation reactions. For a detailed description of the methodology and time-dependent wave packet calculations, the reader is referred to ref 48. The ground and excited-state potential energy surfaces were approximated using harmonic oscillators displaced by Δ in dimensionless normal coordinates. The resonance Raman intensities of the first several overtones as well as the combination bands and the absorption spectrum are determined mainly by the slope of the excited-state surface in the Franck−Condon region in the absence of any vibrational recurrences. The featureless gas and solution phase A-band absorption spectra of cyclopropyl iodide suggests that the total electronic dephasing is mostly from direct photodissociation prior to the first vibrational recurrence. For the resonance Raman bands observed in our experimental spectra, the $\langle f|I(t)\rangle$ overlaps decay and have a negligible value after 30 fs. The effects of solvent dephasing used a simple exponential decay term ($\exp[-t/\tau]$). The bound harmonic oscillator model only provides a convenient method to simulate the Franck−Condon region portion of the excited state surface that determines the resonance Raman intensities and absorption spectrum and does not indicate that the excited state is bound. The simulations only used homogeneous broadening, since this appeared adequate to simulate the resonance Raman partial excitation profile and absorption cross sections. Inhomogeneous broadening may affect the relative intensities of different Raman bands as well as the cross sections. However, a number of previous investigations of A-band alkyl iodides[34b,35b−d,37,40,44] found little need to include substantial inhomogeneous broadening to simultaneously model the resonance Raman partial excitation profile, absolute Raman cross sections, and the absorption band. Thus, we do not expect significant inhomogeneous broadening to be needed to model the A-band absorption and resonance Raman intensities of cyclopropyl iodide.

Density functional theory calculations[54] were done to find the optimized geometry and vibrational frequencies for the ground electronic state of cyclopropyl iodide. Complete geometry optimization and vibrational frequency computations were done analytically using C_S symmetry employing the B3LYP method and the Sadlej-PVTZ basis set contracted as (6s4p//3s2p), (10s6p4d//5s3p2d), and (19s15p12d4f//11s9p6d2f) for the H, C, and I atoms, respectively.[55] This basis set was composed of 290 basis functions contracted from 996 Gaussian functions. The optimization was determined when the maximum force and its root-mean-square (rms) were less than 0.00045 and 0.0003 hartree/bohr, respectively. All of density functional theory calculations made use of the Gaussian program suite.[56]

Results and Discussion

FT-IR and FT-Raman Spectra of Cyclopropyl Iodide. Figure 1 presents a depiction of the geometry of cyclopropyl

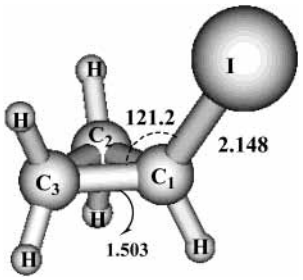

Figure 1. Simple schematic diagram of the geometry of cyclopropyl iodide with the atoms numbered.

TABLE 1: Selected Structural Parameters for Cyclopropyl Iodide

description	length Å	description	angle deg
C1−I	2.148	C1−C2−C3	59.7
C1−C2	1.503	C2−C1−C3	60.5
C2−C3	1.515	C1−C3−C2	59.7
C1−C3	1.515	I−C1−C3	121.2
C1−H1	1.091	I1−C1−C2−C3	110.7
		H4−C3−C1−C2	−106.7

TABLE 2: Experimental FT-IR and FT-Raman Vibrational Bands and Calculated Vibrational Frequencies for Cyclopropyl Iodide from B3LYP/Sadlej-PVTZ

sym	mode	B3LYP/ Sadlej-PVTZ	experimental FT-IR	experimental FT-Raman	assignments
A	ν_1	3221	3081 w	3080 m sh	CH_2 sym stretch
	ν_2	3176	3003 m	3005 s	*CH stretch
	ν_3	3118	2975 vw		CH_2 sym stretch
	ν_4	1471	1443 m	1441 vw sh	CH_2 sym deform
	ν_5	1265	1239 vs	1240 w	sym ring breath
	ν_6	1217	1194 s	1194 m	sym ring breath
	ν_7	1043	1055 w		CH_2 sym twist
	ν_8	1026	1027 s	1028 w	CH_2 sym wag
	ν_9	875	856 m	857 m	sym ring deform
	ν_{10}	746	761 w	759 w	CH_2 sym rock
	ν_{11}	488		492 s	I−C stretch
	ν_{12}	240		244 s	Sym C−I deform
A″	ν_{13}	3207	3052	3054 m	CH_2 asym stretch
	ν_{14}	3112	2975 vw		CH_2 asym stretch
	ν_{15}	1425	1424 m	1426 w	CH_2 asym deform
	ν_{16}	1160	1163 w		CH_2 asym twist
	ν_{17}	1085	1089 w		*CHI asym deform
	ν_{18}	1053	1055 w		CH_2 asym wag
	ν_{19}	929	912 mw	909 w	asym ring deform
	ν_{20}	790	804 m	807 vw	CH_2 asym rock
	ν_{21}	276		284 w sh	asym C−I deform

iodide with the atoms numbered. The optimized geometry was determined for cyclopropyl iodide from B3LYP/Sadlej-PVTZ calculations, and selected structural parameters are listed in Table 1. A gas-phase infrared spectrum of cyclopropyl iodide was obtained some time ago, and to our knowledge this is the only report of a vibrational spectrum for cyclopropyl iodide.[57] Thus, we obtained FT-IR and FT-Raman spectra of the neat cycloproyl iodide that we synthesized. FT-IR and FT-Raman spectra of neat cycloproyl iodide were obtained. Comparison of the FT-IR and FT-Raman spectra shows they have some complementary features that can be useful in making vibrational assignments. The B3LYP/Sadlej-PVTZ calculated vibrational frequencies are readily assigned to the experimental FT-IR and FT-Raman vibrational bands, as shown in Table 2. All 21 fundamental vibrational bands of cyclopropyl iodide have been assigned to vibrational bands observed in either the FT-IR and/or FT-Raman spectra. These tentative vibrational assignments for cyclopropyl iodide were used to assign the Raman bands in the resonance Raman spectra discussed in the next section. Our results are in reasonable agreement with a previous ab initio study of cyclopropyl halides.[58]

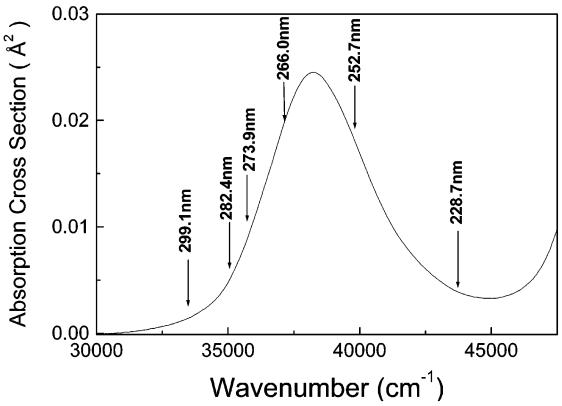

Figure 2. Absorption spectrum of cyclopropyl iodide in cyclohexane solution (solid line). The excitation wavelengths used for the resonance Raman experiments are indicated above the absorption spectrum in nm.

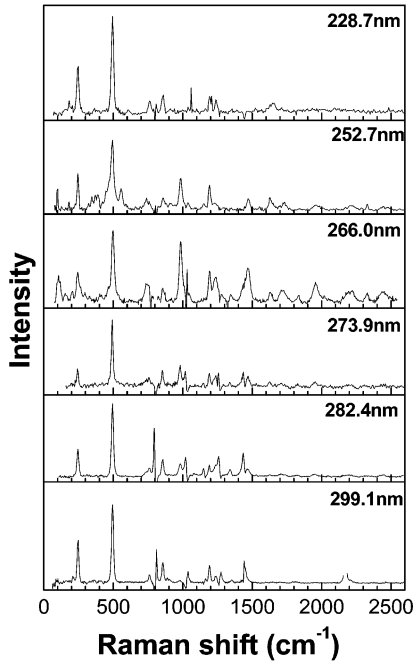

Figure 3. Overall view of the A-band resonance Raman spectra of cyclopropyl iodide in cyclohexane solvent obtained with the excitation wavelengths (in nm) indicated next to each spectrum. The spectra have been intensity-corrected and solvent-subtracted (asterisks mark regions where solvent subtraction artifacts are present).

A-Band Resonance Raman Spectra. Figure 2 shows the absorption spectrum of cyclopropyl iodide in cyclohexane solution. Most of the oscillator strength of the A-band absorption is probably due to the n→σ* transition of $^3Q_0$, as has been determined for methyl iodide and several other related alkyl iodides.[7,8] Our study will focus on elucidating the character of the largest transition and its associated short-time dynamics on the excited-state potential energy surface. The excitation wavelengths used for the resonance Raman experiments are indicated above the absorption spectrum of cyclopropyl iodide shown in Figure 2.

Figure 3 shows an overview of the A-band resonance Raman spectra of cyclopropyl iodide obtained with the excitation wavelengths indicated above the absorption spectrum of Figure 2. Figure 4 presents an expanded view of the resonance Raman spectrum obtained with 266 nm excitation with tentative

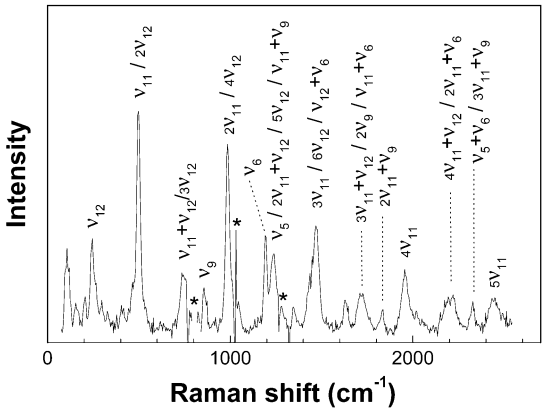

Figure 4. Expanded view of the 266 nm resonance Raman spectrum of cyclopropyl iodide in cyclohexane solvent. The spectrum has been intensity-corrected and solvent-subtracted. Asterisks label parts of the spectrum where solvent-subtraction artifacts are present. The tentative assignments to the larger Raman band features are also shown.

TABLE 3: Parameters for Time-Dependent Wave Packet Calculations for Iodocyclopropane

vibrational mode	ground−state vibrational frequency (cm^{-1})	$\|\Delta\|$
ν_{12} (sym CCI deform)	244	2.0
ν_{11}(C−I stretch)	492	3.3
ν_9 (sym ring deform)	857	0.4
ν_6 (sym ring breath)	1194	0.3

transition length, $M = 0.184$ Å; $E_0 = 34\,750$ cm^{-1}

vibrational assignments indicated above the spectrum. The spectra shown in Figures 3 and 4 have been corrected for sample reabsorption as well as the wavelength dependence response of the detection system. Solvent Raman bands were removed from the spectra by subtracting an appropriately scaled solvent spectrum, and regions with solvent subtraction artifacts are indicated by asterisks. We note that the intensity of some Raman bands in the spectrum may have contributions from several Raman bands that have very close Raman shifts due to the limited resolution of the solution phase spectra. Thus, the Raman band labels in Figure 4 only give the largest Raman band contributions to each Raman feature. Most of the resonance Raman features can be assigned to the fundamentals, overtones, and combination bands of several Franck−Condon active vibrational modes based on our tentative vibrational assignments of cyclopropyl iodide shown in Table 2. This is similar to assignments made for A-band resonance Raman spectra for other alkyl iodides.[34,37,40,44] Inspection of Figure 4 shows that most of the resonance Raman intensity appears in about 14 Raman features assigned to the fundamentals, overtones, and combination bands of four Franck−Condon active modes: the nominal symmetric C−C−I deformation ν_{12} (245 cm^{-1}), the nominal C−I stretch ν_{11} (498 cm^{-1}), the nominal symmetric ring deformation ν_9 (860 cm^{-1}), and the nominal symmetric ring breathing ν_6 (1192 cm^{-1}).

Time-Dependent Wave Packet Calculations To Model the A-band 266 and 252.7 nm Resonance Raman Intensities and Absorption Spectrum. We have chosen to model the relative intensities of the 266 and 252.7 nm resonance Raman spectra, since they are clearly mostly on resonance with the center of the A-band absorption, where the largest transition probably makes the largest contribution as has been found for other alkyl iodides.[34,37,40,44] The 266 and 252.7 nm spectra also have long progressions of overtones and combination bands that should be more indicative of the character of the strong $^3Q_0$ transition. The parameters in Table 3 and the simple model described very briefly in the calculation section of refs 40 and 44 with a simple exponential decay dephasing treatment for the solvent was used to simulate the absorption spectrum and the 266 and 252.7 nm resonance Raman cross sections. Since the A-band resonance Raman spectra of alkyl iodides are susceptible to interference from preresonance-resonance effects[34b] from higher energy states, we have given greater weight to fitting the larger overtones and combination band features. The top of Figure 5 shows a comparison of the calculated absorption spectrum (dotted line) with the experimental (solid line) absorption spectrum. Figure 5 (and Table 4) also show a comparison of the calculated resonance Raman cross sections (open bars) with the experimental Raman cross sections (solid bars) for the 14 main Raman features of the 266 and 252.7 nm resonance Raman spectra.

Inspection of Figure 5 shows that there is reasonable agreement between the calculated absorption spectrum and the experimental one considering that the main $^3Q_0$ transition probably contributes about 70−90% of the oscillator strength of the absorption, as has been found for other A-band alkyl iodide absorption spectra.[7,8] The calculated spectrum fits most of the oscillator strength of the transition while simultaneously providing a good fit to the absolute Raman intensities of the 266 and 252.7 nm spectra as shown in the lower part of Figure 5. If any of the parameters in Table 3 are changed beyond their estimated uncertainties (about ±5−10%), the calculated fit to the absorption spectrum and/or resonance Raman cross section is noticeably poorer. Overall the best fit to both the absorption spectrum and the absolute resonance Raman intensities is reasonable to extract the major features or character of the $^3Q_0$ transition and its associated short-time dynamics on the excited-state potential energy surface. Examination of the $|\Delta|$ dimensionless parameters determined by fitting the absorption spectrum and the resonance Raman cross sections shows that the largest changes in the displacements occur with the nominal C−I stretch mode ν_{11} ($|\Delta| = 3.3$) and the nominal symmetric C−C−I deformation mode ν_{12} ($|\Delta| = 2.0$). There are also more modest contributions from the nominal symmetric ring deformation mode ν_9 ($|\Delta| = 0.4$) and the nominal symmetric ring breathing mode ν_6 ($|\Delta| = 0.3$). Our results indicate that the short-time photodissociation dynamics of cyclopropyl iodide have significant multidimensional character predominantly in the nominal C−I stretch and C−C−I deformation motions accompanied by moderate contributions from the nominal ring deformation and breathing modes.

We note that the intensity of the nominal C−I stretch fundamental of A-band resonance Raman spectra of many alkyl iodides have been found to be significantly affected by preresonance−resonance interference.[18,20,34,35,37,40,44] This preresonance−resonance interference of the C−I stretch fundamental band typically results in the experimental intensity being too low on the low energy side and too high on the high energy side of the absorption band in its middle region compared to the intensity calculated using the basic time-dependent wave packet computations that do not explicitly include the C−I fundamental band preresonance contributions from higher energy states.[18,20,34,35,37,40,44] This is precisely the behavior we observe for the comparison of the intensity of the experimental Raman band feature ($\nu_{11}/2\nu_{12}$) relative to its calculated intensity at 266 and 252.7 nm in Figure 5 and Table 4. Therefore, the discrepancy between the experimental and calculated Raman intensities for the nominal C−I stretch Raman band features ($\nu_{11}/2\nu_{12}$) in the 266 and 252.7 nm spectra is attributed to

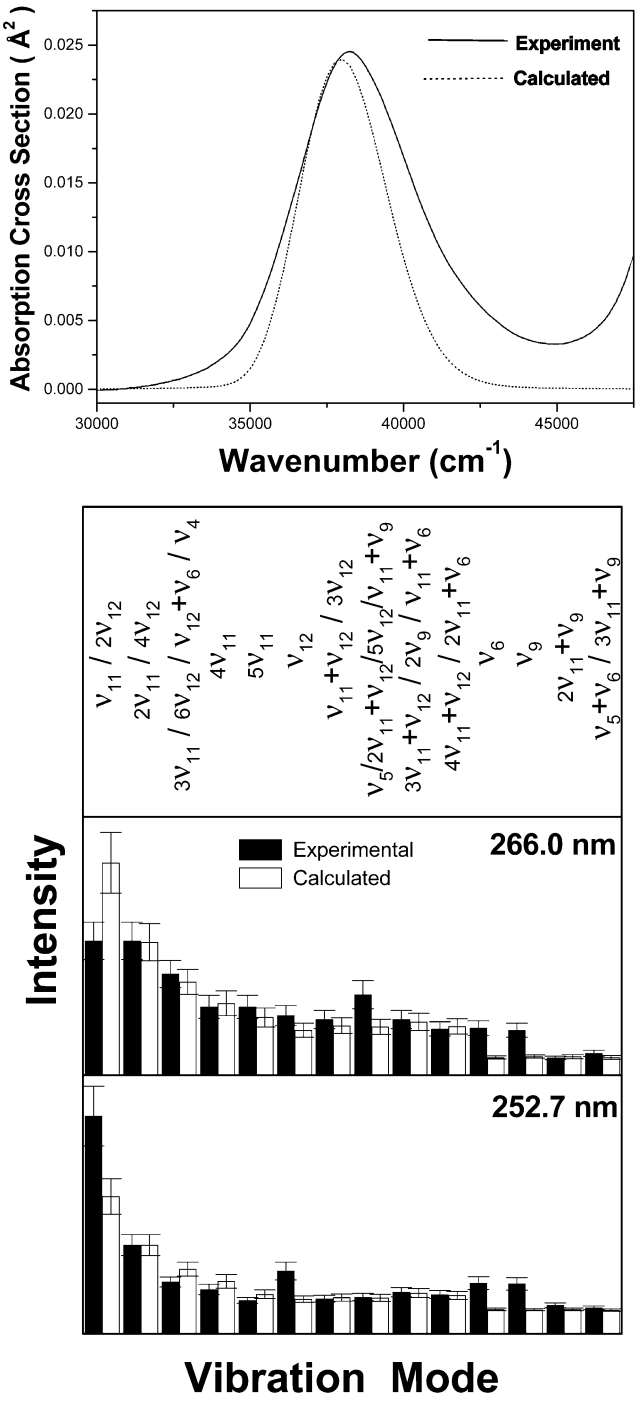

Figure 5. (Top) Comparison of the computed absorption spectrum (dotted line) with the experimental one (solid line). (Bottom) Comparison of the computed resonance Raman cross sections (open bars) with the experimental Raman cross sections (solid bars) for the main Raman features of the 266 and 252.7 nm resonance Raman spectra. The computations made use of the model described in refs 40 and 44 with the simple exponential decay dephasing treatment for the solvent (see the text for details).

preresonance−resonance interference, as has been found for this type of fundamental in many other alkyl iodide resonance Raman spectra.[18,20,34,35,37,40,44]

Comparison of the Franck−Condon Region Short-Time Dynamics of Cyclopropyl Iodide to Other Cyclic Alkyl Iodides and Noncyclic Alkyl Iodides. In Table 5 we compare the normal mode displacements and vibrational reorganizational energies found from the A-band resonance Raman spectra of cyclopropyl iodide to those previously found for the conformers

TABLE 4: Resonance Raman Intensities of Cyclopropyl Iodide in Cyclohexane Solution

		absolute Raman cross section (10^{-9} Å/molecule)			
	Raman shift	266.0 nm		252.7 nm	
Raman band	(cm^{-1})	expt	calcd	expt	calcd
$2\nu_{12}/\nu_{11}$	498	0.3	0.489	0.54	0.322
$2n_{11}/\nu_{12}$	986	0.3	0.297	0.19	0.19
$6\nu_{12}/3\nu_{11}/\nu_{12}+\nu_6/\nu4$	1470	0.22	0.201	0.09	0.125
$4\nu_{11}$	1955	0.14	0.149	0.07	0.092
$5\nu_{11}$	2447	0.14	0.115	0.05	0.057
ν_{12}	245	0.12	0.084	0.12	0.044
$3\nu_{12}/\nu_{11}+\nu_{12}$	735	0.11	0.095	0.045	0.048
$5\nu_{12}/\nu_5/2\nu_{11}+\nu_{12}/\nu_{11}+\nu_9$	1237	0.17	0.092	0.049	0.047
$2\nu_9/3\nu_{11}+\nu_{12}/\nu_{11}+\nu_6$	1710	0.11	0.104	0.062	0.06
$4\nu11+\nu12/2\nu_{11}+\nu_6$	2220	0.087	0.093	0.056	0.054
ν_6	1192	0.089	0.018	0.087	0.016
ν_9	860	0.084	0.02	0.085	0.015
$2\nu_{11}+\nu_9$	1840	0.017	0.02	0.027	0.016
$\nu_5+\nu_6/3\nu_{11}+\nu_9$	2330	0.028	0.018	0.02	0.014

of cyclopentyl iodide and *n*-propyl iodide.[40,44] Examination of Table 5 shows that the total vibrational organizational energy associated with the A-band $^3Q_0$ transition of cyclopropyl iodide is relatively small (about 3325 cm^{-1}) compared to the noncyclic *n*-propyl iodide conformers (about 9070 cm^{-1} for the trans conformer and about 9570 cm^{-1} for the gauche conformer). However, the total vibrational reorganizational energy for cyclopropyl iodide is similar to those found for the cyclopentyl iodide conformers (about 4840 cm^{-1} for axial and 3430 cm^{-1} for equatorial). We note that cyclopropyl iodide generally has smaller normal mode displacements and associated vibrational reorganizational energies in the nominal C−I stretch mode and nominal C−C−I deformation mode (the C−C−C and/or C−C−I modes in *n*-propyl iodide) than found in *n*-propyl iodide. For example, the nominal C−I stretch mode has $|\Delta| = 3.3$ and a vibrational reorganizational energy of 2710 cm^{-1} for cyclopropyl iodide compared to $|\Delta| = 3.76$ ($|\Delta| = 5.62$) and vibrational reorganizational energies of 4200 cm^{-1} (7975 cm^{-1}) for trans (gauche) *n*-propyl iodide.[40] Similarly, cyclopropyl iodide has only one low-frequency mode, the nominal C−C−I deformation at 245 cm^{-1} that has $|\Delta| = 2.0$ and a vibrational reorganizational energy of 490 cm^{-1} compared to two corresponding low-frequency modes (the nominal C−C−C and C−C−I modes) in the 200−300 cm^{-1} region for the *n*-propyl iodide conformations that have $|\Delta| = 4.50$ and 4.40 with vibrational reorganizational energies of 2926 and 1946 cm^{-1} respectively for the trans conformer and $|\Delta| = 2.51$ and 1.90 with vibrational reorganizational energies of 1228 and 363 cm^{-1}, respectively, for the gauche conformer.[40] It is clear that less energy goes into excitation of both the nominal C−I stretch mode and C−C−I deformation mode of cyclopropyl iodide compared to the corresponding type of modes in the noncyclic *n*-propyl iodide conformers.[40] This is consistent with previous results for the conformers of cyclopentyl iodide that found substantially less total vibrational energy in these types of modes in the 200−700 cm^{-1} range and less change in the C−I bond length and C−C−I bond angles at 10 fs compared to the *n*-propyl iodide conformers.[44] This and our present results for cyclopropyl iodide indicate that the A-band Franck−Condon photodissociation dynamics of cyclic alkyl iodides have less excitation or motion in the C−C−I bending motions compared to their corresponding noncylcic alkyl iodides. Thus, the cyclic backbone appears to restrict the C−I bond cleavage along the CCI bending motions compared to their noncyclic alkyl iodide counterparts.

TABLE 5: Comparison of Normal Mode Displacements and Vibrational Reorganization Energies Found for the A-band Resonance Raman Spectra of Cyclopropyl Iodide (This Work), Cyclopentyl Iodide,[44] and 1-Propyl Iodide[40]

vibrational mode	ground-state vibrational frequency (cm^{-1})	$\|\Delta\|$	vibrational reorganization energy (cm^{-1})
	Cyclopropyl Iodide		
ν_{12} (sym C−C−I deform)	244	2.0	490
ν_{11} (C−I stretch)	492	3.3	2712
ν_9 (sym ring deform)	857	0.4	69
ν_6 (sym ring breath)	1194	0.3	54
transition length, $M = 0.184$ Å; $E_0 = 34\,750$ cm^{-1}			total 3325
	1-Iodopropane		
	Trans Conformation		
ν_{14} C−I stretch	594	3.76	4199
ν_{15} C−C−C bend	289	4.50	2926
ν_{16} C−C−I bend	201	4.4	1946
transition length, $M = 0.196$ Å; $E_0 = 29\,720$ cm^{-1}; $\Gamma = 40$ cm^{-1}			total 9071
	Gauche Conformation (Three-Mode Calculation)		
ν_{23} C−I stretch	505	5.62	7975
ν_{24} C−C−C bend	390	2.51	1228
ν_{25} C−C−I bend	201	1.90	363
transition length, $M = 0.193$ Å; $E_0 = 29\,720$ cm^{-1}; $\Gamma = 70$ cm^{-1}			total 9566
	Iodocyclopentane		
	Axial Conformer		
ν_{11}, γ-CH_2 twist	1190	0.23 ± 0.02	31
ν_{12}, α-CH bend	1094	0.30 ± 0.03	49
ν_{13}, ring deformation	1034	0.50 ± 0.05	129
ν_{15}, β-CH_2 rock	903	0.57 ± 0.05	147
ν_{18}, C−I stretch	672	0.91 ± 0.05	278
ν_{19}, C−I stretch	481	3.75 ± 0.18	3382
ν_{20}, C−C−C bend	286	2.40 ± 0.10	825
			total 4840
	Equatorial Conformer		
ν_8, β-CH_2 wag	1308	0.27 ± 0.03	48
ν_{11}, γ-CH_2 twist	1190	0.38 ± 0.03	86
ν_{12}, α-CH bend	1110	0.30 ± 0.03	50
ν_{13}, ring deformation	1026	0.35 ± 0.04	63
ν_{16}, γ-CH_2 rock	876	0.57 ± 0.06	142
ν_{18}, C−I stretch	693	0.78 ± 0.08	211
ν_{19}, C−I stretch	430	1.20 ± 0.12	310
ν_{20}, C−C−C bend	249	5.25 ± 0.25	3431
			total 4341

It is interesting to note that there is significant intensity in the fundamental and combination bands of the nominal symmetric ring deformation and ring breathing modes (ν_9 and ν_6, respectively) with the C−I stretch mode (ν_{11}) in the A-band resonance Raman spectra of cyclopropyl iodide. Similar corresponding modes in the 800−1200 cm^{-1} region of cyclopentyl iodide and cyclohexyl iodide also have significant intensity in the fundamentals of these Raman bands and their combination bands with the nominal C−I stretch progression in the A-band resonance Raman spectra of cyclopentyl iodide and cyclohexyl iodide.[43,44] This appears to correlate with the cyclic backbone restricting the C−I bond cleavage along the CCI bending motions, since these fundamentals and combination bands appear to be very weak in the *n*-propyl iodide A-band resonance Raman spectra relative to the low-frequency C−I stretch and C−C−I/C−C−C bending progressions.[40,44] In fact, the more detailed study on the cyclopentyl iodide molecule found that the C−C bonds are stretched substantially more at 10 fs (about 0.0455 Å for axial and 0.021 Å for equatorial C−C bonds, where one C is the one attached to the I atom)[44] than the corresponding C−C bond in *n*-propyl iodide (only −0.005 to −0.011 Å for trans and +0.005−0.006 Å for gauche).[40] The similarity in the cyclopropyl iodide and cyclopentyl iodide A-band resonance Raman combination bands of the ring deformation/breathing modes in the 800−1200 cm^{-1} region with the nominal C−I stretch modes suggests that the Franck−Condon region photodissociation dynamics of cyclopropyl iodide also undergo relatively large changes in the C−C bonds, becoming longer like cyclopentyl iodide. This is consistent with the ab initio results of Arnold et al.[45] that indicate the C−I bond cleavage is accompanied by a noticeable increase in the C−C bond distance (or weakening of the C−C bond). This appears to allow the molecule to more easily reach the curve crossing between the open-shell and closed-shell potential energy surfaces that enables direct formation of allyl radical product.[45] The restriction of the cyclic backbone in cyclic alkyl iodides such as cyclopropyl iodide and cyclopentyl iodide appears to lead to more change in the C−C bond, with the bond becoming noticeably longer during the Franck−Condon region dynamics compared to *n*-alkyl iodides such as *n*-propyl iodide.[34b,40]

It is also interesting to compare previous A-band resonance Raman intensity analysis results for isopropyl iodide[34b,37] and *n*-propyl iodide[40] to those for cyclic alkyl iodides such as cyclopropyl iodide and cyclopentyl iodide.[44] This comparison can help to better understand the similarities and differences in the behavior of the A-band Franck−Condon region C−C bond length changes in the *n*-alkyl iodides versus the cyclic alkyl iodides and secondary or tertiary noncyclic iodides. The ground state structures of isopropyl iodide and cyclopropyl iodide are qualitatively similar, except the C−C−C angle is noticeably smaller due to the cyclopropyl ring. In both molecules the C−I bond has a similar position relative to the three C atoms. As the C−I bond begins to break in the Franck−Condon region, this pushes the carbon atom attached to the iodine atom away from the other two C atoms and leads to noticeably longer C−C bond lengths (estimated to be +0.03−0.05 Å at 10 fs in isopropyl iodide).[37] This situation is very similar to the C−I bonds in cyclic alkyl iodides in that the initial C−I bond cleavage pushes the C atom that the iodine is attached to away from the other nearest C atoms (β-position ones) so as to make these C−C bonds longer (estimated to be +0.0455 Å for axial and +0.021 Å for equatorial C−C bonds in cyclopentyl iodide, for example).[44] However, the different orientation of the C−I bond in the *n*-alkyl iodides relative to the alkyl fragment leads to the C−I bond cleavage to put more energy into rotation of the α-C atom relative to the alkyl chain and appears to lead to either a smaller C−C bond or only a very modest lengthening of the C−C bond in the Franck−Condon region (estimated to be only −0.005 to −0.011 Å for trans and +0.005−0.006 Å for gauche in *n*-propyl iodide).[40] Thus, the C−I bond cleavage in the Franck−Condon region appears to give longer bond lengths for the C−C bonds where one C atom is attached to the I atom in cyclic alkyl iodides such as cyclopentyl iodide[44] and cyclopropyl iodide as well as alkyl iodides, where the I atom is attached to a substituted carbon atom such as in isopropyl iodide or *tert*-butyl iodide compared to *n*-alkyl iodides such as *n*-propyl iodide[40] or ethyl iodide.[37]

If the proposed open shell−closed shell curve crossing mechanism for cyclopropyl iodide (where one needs both significant C−I and C−C bond lengthening) occurs in a similar manner for other alkyl iodides, then we speculate that the efficiency of curve crossing may vary noticeably with the structure of the alkyl iodide. For example, *n*-propyl iodide A-band photodissociation appears to lead to little excitation or

lengthening of the C−C bond so this may not be able to approach a surface crossing requiring significant displacements in both the C−I and C−C bond lengths. However, cyclic alkyl iodides such as cyclopentyl iodide and cyclopropyl iodide that have significant displacements of both the C−I and C−C bond lengths will be able to efficiently approach a surface crossing requiring noticeable displacements in the C−I and C−C bond lengths. More work is needed to see if this is actually the case and to better understand how the proposed open shell−closed shell curve crossings may affect the photochemistry of cyclic and noncyclic alkyl iodides and alkyl halides in general. As Arnold et al.[45] pointed out earlier, femtosecond time-resolved experiments would be helpful to learn more about the pathway(s) responsible for formation of the allyl radical in the gas and solution phases. Such experiments would help bridge the gap between the initial Franck−Condon region dynamics and the final products observed after photoexcitation. In addition, a wide variety of both experimental work and theoretical work is needed to understand the details of the formation of different products produced after ultraviolet photoexcitation of alkyl halides in the gas and solution phases.

Conclusions

A-band resonance Raman spectra were acquired for cyclopropyl iodide in cyclohexane solution, and a preliminary resonance Raman intensity analysis was done. The resonance Raman spectra and intensity analysis indicate that most of the short-time photodissociation dynamics in the Franck−Condon region occurs along the nominal C−I stretch and nominal C−C−I deformation normal modes and smaller components along the nominal cyclopropyl ring deformation and breathing normal modes. These results for cyclopropyl iodide were compared to those previously reported for several cyclic and noncyclic alkyl iodides. The vibrational reogranizational energies and short-time dynamics for cyclopropyl iodide were very similar to those found for cyclopentyl iodide and somewhat different than those for *n*-propyl iodide. This similarity combined with previous results for cyclopentyl suggests that the Franck−Condon region photodissociation dynamics of cyclopropyl iodide also have relatively large changes in the C−C bonds becoming longer as found in cyclopentyl iodide. This is consistent with the ab initio results of Arnold et al.[45] that indicate that the C−I bond cleavage is accompanied by a noticeable increase in the C−C bond distance (or weakening of the C−C bond). Cyclic alkyl iodides such as cyclopropyl iodide and cyclopentyl iodide appear to have somewhat more change in the C−C bond, with the bond becoming noticeably longer during the Franck−Condon region dynamics compared to *n*-alkyl iodides such as *n*-propyl iodide.[34b,40]

Acknowledgment. This work was supported by grants from the Zhejiang Provincial Natural Science Foundation of China and the Zhejiang Provincial Instrumental Analysis Fund of China to X.Z. and from the Research Grants Council (RGC) of Hong Kong (HKU 7087/01P) to D.L.P.

References and Notes

(1) Riley, S. J.; Wilson, K. R. *Faraday Discuss. Chem. Soc.* **1972**, *53*, 132.
(2) Sparks, R. K.; Shobatake, K.; Carlson, L. R.; Lee, Y. T. *J. Chem. Phys.* **1981**, *75*, 3838.
(3) Van Veen, G. N. A.; Baller, T.; Devries, A. E.; Van Veen, N. J. A. *Chem. Phys.* **1984**, *87*, 405.
(4) Godwin, F. G.; Paterson, C.; Gorry, P. A.; *Mol. Phys.* **1987**, *61*, 827.
(5) Black, J. F.; Powis, I. *Chem. Phys.* **1988**, *125*, 375.
(6) Zhu, Q.; Cao, J. R.; Wen, Y.; Zhang, J.; Huang, Y.; Fang, W.; Wu, X. *Chem. Phys. Lett.* **1988**, *144*, 486.
(7) Gedanken, A.; Rowe, M. D. *Chem. Phys. Lett.* **1975**, *34*, 39.
(8) Gedanken, A. *Chem. Phys. Lett.* **1987**, *137*, 462.
(9) Donohue, T.; Wiesenfeld, J. *J. Chem. Phys.* **1975**, *63*, 3130.
(10) Brewer, P.; Das, P.; Ondrey, G.; Bersohn, R. *J. Chem. Phys.* **1983**, *79*, 720.
(11) Hess, W. P.; Kohler, S. J.; Haugen, H. K.; Leone, S. R. *J. Chem. Phys.* **1986**, *84*, 2143.
(12) Ogorzalek-Loo, R.; Hall, G. E.; Haerri, P.; Houston, P. L. *J. Phys. Chem.* **1987**, *92*, 5.
(13) Knee, J. L.; Khundar, L. R.; Zewail, A. H. *J. Chem. Phys.* **1985**, *83*, 1996.
(14) Ogorzalek-Loo, R.; Haerri, H.-P.; Hall, G. E.; Houston, P. L. *J. Chem. Phys.* **1989**, *90*, 4222.
(15) Chandler, D. W.; Janssen, M. H. M.; Stolte, S.; Strickland, R. N.; Thoman, J. W. Jr.; Parker, D. H. *J. Phys. Chem.* **1990**, *94*, 4839.
(16) Triggs, N. E.; Zahedi, M.; Nibler, J. W.; Debarber, P. A.; Valentini, J. J. *J. Chem. Phys.* **1992**, *96*, 2756.
(17) Mastenbroek, J. W. G.; Taatjes, C. A.; Nauta, K.; Janssen, M. H. M. Stolte, S. *J. Phys. Chem.* **1995**, *99*, 4360.
(18) Galica, G. E.; Johnson, B. R.; Kinsey, J. L.; Hale, M. O. *J. Phys. Chem.* **1991**, *95*, 7994.
(19) Lao, K. Q.; Person, M. D.; Xayaroboun, P.; Butler, L. J. *J. Chem. Phys.* **1990**, *92*, 823.
(20) Markel, F.; Myers, A. B. *J. Chem. Phys.* **1993**, *98*, 21.
(21) Duschek, F.; Schmitt, M.; Vogt, P.; Materny, A.; Kiefer, W. *J. Raman Spectrosc.* **1997**, *28*, 445.
(22) Shapiro, M.; Bersohn, R. *J. Chem. Phys.* **1980**, *72*, 3810.
(23) Guo, H.; Schatz, G. C. *J. Chem. Phys.* **1991**, *95*, 3091.
(24) Hammerich, A. D.; Manthe, U.; Kosloff, R.; Meyer, H.-D.; Cederbaum, L. S. *J. Chem. Phys.* **1994**, *101*, 5623.
(25) Amatatsu, Y.; Yabushita, S.; Morokuma, K. *J. Chem. Phys.* **1996**, *104*, 9783.
(26) (a) Dzvonik, M. K.; Yang, S.; Bersohn, R. *J. Chem. Phys.* **1974**, *61*, 4408. (b) Kawasaki, M.; Lee, S. J.; Bersohn, R. *J. Chem. Phys.* **1975**, *63*, 809.
(27) Kroger, P. M.; Demou, P. C.; Riley, S. J. *J. Chem. Phys.* **1976**, *65*, 1823.
(28) Krajnovitch, D.; Butler, L. J.; Lee, Y. T. *J. Chem. Phys.* **1984**, *81*, 3031.
(29) Xu, Q.-X.; Jung, K.-H.; Bernstein, R. B. *J. Chem. Phys.* **1988**, *89*, 2099.
(30) (a) Kang, W. K.; Jung, K. W.; Kim, D. C.; Jung, K.-H.; Im, H. S. *Chem. Phys.* **1995**, *196*, 363. (b) Kang, W. K.; Jung, K. W.; Kim, D.-C.; Jung, K.-H. *J. Chem. Phys.* **1995**, *104*, 5815.
(31) Fairbrother, D. H.; Briggman, K. A.; Wietz, E.; Stair, P. C. *J. Chem. Phys.* **1994**, *101*, 3787.
(32) (a) Uma, S.; Das, P. K. *Chem. Phys. Lett.* **1995**, *241*, 335. (b) Uma, S.; Das, P. K. *J. Chem. Phys.* **1996**, *104*, 4470.
(33) Zhang, J.; Imre, D. G. *J. Chem. Phys.* **1988**, *89*, 309.
(34) (a) Phillips, D. L.; Lawrence, B. A.; Valentini, J. J. *J. Phys. Chem.* **1991**, *95*, 9085. (b) Phillips, D. L.; Myers, A. B. *J. Chem. Phys.* **1991**, *95*, 226. (c) Phillips, D. L.; Valentini, J. J.; Myers, A. B. *J. Phys. Chem.* **1992**, *96*, 2039.
(35) (a) Man, S. Q.; Kwok, W. M.; Phillips, D. L. *J. Phys. Chem.* **1995**, *99*, 15705. (b) Kwok, W. M.; Phillips, D. L. *J. Chem. Phys.* **1996**, *104*, 2529. (c) Kwok, W. M.; Phillips, D. L. *J. Chem. Phys.* **1996**, *104*, 9816. (d) Man, S.-Q.; Kwok, W. M.; Johnson, A. E.; Phillips, D. L. *J. Chem. Phys.* **1996**, *105*, 5842.
(36) Kwok, W. M.; Ng, P. K.; He, G. Z.; Phillips, D. L. *Mol. Phys.* **1997**, *90*, 127.
(37) Phillips, D. L.; Myers, A. B. *J. Raman Spectrosc.* **1997**, *28*, 839.
(38) Zheng, X.; Phillips, D. L. *Chem. Phys. Lett.* **1998**, *286*, 79.
(39) Zheng, X.; Phillips, D. L. *Chem. Phys. Lett.* **1998**, *292*, 295.
(40) Zheng, X.; Phillips, D. L. *J. Chem. Phys.* **1998**, *108*, 5772.
(41) Zheng, X.; Phillips, D. L. *Chem. Phys. Lett.* **1999**, *307*, 350.
(42) Freitas, J. E.; Hwang, H. J.; Tricknor, A. B.; El-Sayed, M. A. *Chem. Phys. Lett.* **1991**, *183*, 165.
(43) Zheng, X.; Phillips, D. L. *Chem. Phys. Lett.* **1998**, *296*, 173.
(44) Zheng, X.; Lee, C. W.; Phillips, D. L. *J. Chem. Phys.* **1999**, *111*, 11034.
(45) Arnold, P. A.; Cosofret, B. R.; Dylewski, S. M.; Houston, P. L.; Carpenter, B. K. *J. Phys. Chem. A* **2001**, *105*, 1693.
(46) (a) Heller, E. J. *J. Chem. Phys.* **1975**, *62*, 1544, (b) Lee, S. Y.; Heller, E. J. *J. Chem. Phys.* **1979**, *71*, 4777, (c) Heller, E. J.; Sundberg, R. L.; Tannor, D. J. *J. Phys. Chem.* **1982**, *86*, 1822.
(47) (a) Ziegler, L. D.; Albrecht, A. C. *J. Chem. Phys.* **1979**, *70*, 2644. (b) Ziegler, L. D.; Albrecht, A. C. *J. Chem. Phys.* **1979**, *70*, 2634. (c) Ziegler, L. D.; Hudson, B. *J. Chem. Phys.* **1981**, *74*, 982. (d) Ziegler, L. D.; Hudson, B. *J. Chem. Phys.* **1983**, *79*, 1197. (e) Ziegler, L. D.; Hudson, B. *J. Chem. Phys.* **1983**, *79*, 1134.
(48) (a) Myers, A. B.; Mathies, R. A. In *Biological Applications of Raman Spectroscopy*; Spiro, T. G., Ed.; Wiley: New York, 1987; Vol. 2, p 1. (b) Myers, A. B. In *Laser Techniques in Chemistry*; Myers, A. B.,

Rizzo, T. R., Eds.; Wiley: New York, 1995; p 325. (c) Myers, A. B. *Chem. Rev.* **1996**, *96*, 911.

(49) (a) Waterland, M. R.; Kelley, A. M. *J. Phys. Chem. A* **2001**, *105*, 8385. (b) Leng, W. A.; Kelley, A. M. *Langmuir* **2003**, *19*, 7049.

(50) (a) Tauber, M. J.; Mathies, R. A. *J. Phys. Chem. A* **2001**, *105*, 10952. (b) Tauber, M. J.; Mathies, R. A. *J. Am. Chem. Soc.* **2003**, *125*, 1394.

(51) (a) Webb, M. A.; Loppnow, G. R. *J. Phys. Chem. A* **1999**, *103*, 6283, (b) Webb, M. A.; Loppnow, G. R. *J. Phys. Chem. B* **2002**, *106*, 2102. (c) Fraga, E.; Loppnow, G. R. *J. Phys. Chem. B* **2002**, *106*, 10474.

(52) (a) Reid, P. J. *Acc. Chem. Res.* **2001**, *34*, 691. (b) Reid, P. J. *J. Phys. Chem. A* **2002**, *106*, 1473, (c) Barham, B. P.; Reid, P. J. *Chem. Phys. Lett.* **2002**, *361*, 49.

(53) (a) Biswas, N.; Umapathy, S. *J. Chem. Phys.* **1997**, *107*, 7849, (b) Biswas, N.; Abraham, B.; Umapathy, S. *J. Phys. Chem. A* **2002**, *106*, 9397, (c) Biswas, N.; Umapathy, S. *J. Chem. Phys.* **2003**, *118*, 5526.

(54) (a) Becke, A. *J. Chem. Phys.* **1986**, *84*, 4524. (b) Lee, C.; Yang, W.; Parr, R. G. *Phys. Rev. B* **1988**, *58*, 785.

(55) Sadlej, A. J. *Theor. Chem. Acta* **1992**, *81*, 339.

(56) Gaussian 98, Revision A.7, Frisch, M. J.; Trucks, G. W.; Schlegel, H. B.; Scuseria, G. E.; Robb, M. A.; Cheeseman, J. R.; Zakrzewski, V. G.; Montgomery, Jr. J. A.; Stratmann, R. E.; Burant, J. C.; Dapprich, S.; Millam, J. M.; Daniels, A. D.; Kudin, K. N.; Strain, M. C.; Farkas, O.; Tomasi, J.; Barone, V.; Cossi, M.; Cammi, R.; Mennucci, B.; Pomelli, C.; Adamo, C.; Clifford, S.; Ochterski, J.; Petersson, G. A.; Ayala, P. Y.; Cui, Q.; Morokuma, K.; Malick, D. K.; Rabuck, A. D.; Raghavachari, K.; Foresman, J. B.; Cioslowski, J.; Ortiz, J. V.; Baboul, A. G.; Stefanov, B. B.; Liu, G.; Liashenko, A.; Piskorz, P.; Komaromi, I.; Gomperts, R.; Martin, R. L.; Fox, D. J.; Keith, T.; Al-Laham, M. A.; Peng, C. Y.; Nanayakkara, A.; Gonzalez, C.; Challacombe, M.; Gill, P. M. W.; Johnson, B.; Chen, W.; Wong, M. W.; Andres, J. L.; Gonzalez, C.; Head-Gordon, M.; Replogle, E. S.; Pople, J. A.; Gaussian, Inc., Pittsburgh, PA, 1998.

(57) Hirokawa, T.; Hayashi, M.; Murata, H. *J. Sci. Hiroshima University A* **1973**, *37*, 301.

(58) Kaupert, C.; Heydtmann, H.; Thiel, W. *Chem. Phys.* **1991**, *156*, 85.